Adsorption and structural environment of Co(II) at the zinc oxide- and zinc sulfide-aqueous solution interfaces

ARTICLE *in* LANGMUIR · OCTOBER 1995

Impact Factor: 4.46 · DOI: 10.1021/la00010a032

3 AUTHORS, INCLUDING:

Per Persson
Lund University
144 PUBLICATIONS **4,105** CITATIONS

Adsorption and Structural Environment of Co(II) at the Zinc Oxide– and Zinc Sulfide–Aqueous Solution Interfaces

P. Persson,*,† G. A. Parks,‡ and G. E. Brown, Jr.‡

Department of Inorganic Chemistry, Umeå University, S-901 87, Sweden, and Surface and Aqueous Geochemistry Group, Department of Geological and Environmental Sciences, Stanford University, Stanford, California 94305-2115

Received March 29, 1995. In Final Form: May 30, 1995®

Adsorption of Co(II) at the aqueous interfaces of ZnO and ZnS (wurtzite) has been studied by classical wet-chemical methods, and the structure and composition of Co adsorption complexes at these interfaces have been determined by *in-situ* X-ray absorption fine structure (XAFS) spectroscopy. On both adsorbents, adsorption as a function of pH shows the normal behavior, i.e., a pronounced adsorption within a relatively narrow pH range. There is no evidence for ion exchange between Zn and Co on either of the solids, indicating that uptake must be due to surface complexation or surface precipitation. By use of log(IAP) ($IAP = a_{Co(II)}a_{OH^-}{}^{-2}$) vs pH diagrams, the maximum surface complex binding capacities of Co(II) on ZnO and ZnS were estimated to be 2.5 and 2.0 μmol/m^2, respectively. At the molecular level, the XAFS results show the presence of both four- and six-coordinated oxygen-ligated Co(II) on ZnO, corresponding to Co–O distances of 1.95 and 2.10 Å. On ZnS, two Co–O distances are also indicated and a Co–S correlation is observed at 2.36 Å. These spectroscopic results, together with the wet-chemical data, show that the Co–S correlation is due to surface complexation of Co(II) to sulfide sites. Higher shell EXAFS analysis indicates that Co(II) adsorbs to defect structural positions where Zn atoms are missing at the surface. On ZnO these Co(II) surface complexes are slightly distorted as compared to the ZnO bulk structure, while almost no distortions are observed for Co(II) surface complexes on ZnS. At increased Co(II) coverages, a structurally disordered $Co(OH)_2$ phase is formed on both adsorbents. The disorder is shown to be of a short- to medium-range nature, i.e., disorder within 4–5 Å radius of the central Co atoms as compared to crystalline $Co(OH)_2$, and is observed even at the high surface coverage of 42.1 μmol/m^2 on ZnS.

Introduction

Adsorption reactions of metal ions on hydrated solid surfaces are frequently encountered, both in the natural aquatic environment and in industrial processes. As a consequence, numerous studies have been devoted to this field of surface science, and theories for describing the macroscopic behavior of liquid–solid systems have been developed.[1] In particular, the coordination chemistry approach has been successfully applied to explain the interactions of cations and anions, at or below monolayer coverages, at the aqueous–oxide interface.[2] This approach is based on the assumption that a hydrated metal oxide surface is comprised of $\underline{S}M-OH$ groups ($\underline{S}$ denotes a solid surface), which can accept and donate protons. In other words the oxide surface behaves as a protic acid, usually characterized by two overall pK-values which describe a protonation and a deprotonation reaction to $\underline{S}M-OH_2^+$ and $\underline{S}M-O^-$, respectively. Furthermore, the surface oxygen atoms can act as Lewis bases toward incoming acids, and the surface metal atoms can accordingly act as Lewis acids toward bases. Thus, adsorption or surface complexation reactions can be described in the same terms as coordinative interactions in homogenous aqueous solution. In aqueous solution, factors such as the size, charge and structure of the central ion and the ligands, pH, and ionic strength influence complex formation. The same is true for processes at an interface, but in this case the overall charge, structure (both geometric and electronic), composition, and morphology of the surface can also have an effect on the stability and structure of the species formed. To understand how the various factors affect surface complexation and to properly formulate the reactions in surface coordination chemistry models, microscopic structural and compositional information is needed for surface complexes at aqueous solution–solid interfaces.

Until recently, structural investigations of adsorbates at the aqueous solution–solid interface were scarce. This was primarily due to the fact that most surface analytical techniques involve drying the sample and transferring it to a high-vacuum environment.[3] Thus, these techniques provide only indirect information, which might be difficult to relate to a state with water present. Within the past decade spectroscopic methods have been applied which allow *in-situ* characterization, i.e., with bulk water in contact with the solid surface. In particular, synchrotron-based X-ray absorption spectroscopy, XAS, has proven to be a powerful *in-situ* probe for determining the structure and bonding of adsorbates at the aqueous solution–solid interface.[3-9] XAS, which is an element specific technique, offers the possibility of characterizing the local structural environment around an adsorbed ion, i.e., distances to, coordination numbers of, and chemical identities of neighbors within ~4–5 Å radius. In the present study

† Umeå University.
‡ Stanford University.
® Abstract published in *Advance ACS Abstracts,* August 15, 1995.

(1) Adamson, A. W. *Physical Chemistry of Surfaces*, 5th ed.; John Wiley & Sons: New York, 1990.
(2) Stumm, W. *Chemistry of the Solid-Water Interface*; John Wiley & Sons: New York, 1992.
(3) Brown, G. E., Jr., *Mineral-Water Interface Geochemistry, Reviews in Mineralogy*, Hochella, M. F., Jr., White, A. F., Eds.; Mineralogical Society of America: Washington DC, 1990; Vol. 23, pp 309–363.
(4) Chisholm-Brause, C. J.; O'Day, P. A.; Brown, G. E., Jr.; Parks, G. A. *Nature* **1990,** *348,* 528–531.
(5) O'Day, P. A.; Brown, G. E., Jr.; Parks, G. A. *J. Colloid Interface Sci.* **1994,** *165,* 269–289.
(6) Manceau, A.; Charlet, L. *J. Colloid Interface Sci.* **1992,** *148,* 425–442.
(7) Charlet, L.; Manceau, A. *J. Colloid Interface Sci.* **1992,** *148,* 443–458.
(8) O'Day, P. A. Structure, *Bonding, and Site Preference of Cobalt(II) Sorption Complexes on Kaolinite and Quartz from Solution and Spectroscopic Studies*, Ph.D. Thesis, Stanford University, 1992.
(9) Xu, N. *Spectroscopic and Solution Chemistry Studies of Cobalt-(II) Sorption Mechanisms at the Calcite-Water Interface*, Ph.D. Thesis, Stanford University, 1993.

0743-7463/95/2411-3782$09.00/0

we have examined the adsorption of aqueous Co(II) on ZnO and ZnS (wurtzite), using XAS together with wet-chemical batch titrations. Our objective was to examine the effect of substrates of different chemical composition but with the same general structure on adsorption reactions of hydrated metal ions. These systems are of interest from a coordination chemistry point of view since ZnO has SZn−OH sites available for coordination while ZnS has possibly both SZn−OH and SZn−SH sites. Co(II) was chosen as the adsorbate for three main reasons: (1) Several XAS studies have been performed previously on aqueous Co(II) adsorption on oxide, clay, and calcite surfaces, and therefore much is known about the surface coordination chemistry of Co(II).[4,5,8,9] (2) Co(II) usually has its so-called adsorption edge in a pH interval (7.5−8.2) which is relatively close to the pH of minimum solubility of ZnO (ca. 9), thus minimizing dissolution of the sorbent.[10] (3) The aqueous solubility of ZnS is on the same order as the solubilities of the Co(II) sulfides;[11] thus surface complex formation might be favored over adsorption via a cation-exchange mechanism and formation of a new sulfide phase. Although metal ions at sulfide surfaces have been analyzed by means of the XAS technique in previous studies,[12] the present XAS study is, to our knowledge, the first on metal ions at the *aqueous solution*−sulfide interface.

Experimental Section

Adsorbents. The ZnO and ZnS used in this study were reagent grade materials obtained from Aldrich. The wurtzite-type structural identity of the adsorbents was confirmed by X-ray diffraction. The powders were analyzed with X-ray photoelectron spectroscopy (XPS) and with diffuse reflectance (DR) Fourier transform infrared (FTIR) spectroscopy. ZnO proved to be free from impurities, within the detection limits of the techniques, and was used in the experiments without any pretreatment. ZnS contained substantial surface impurities of $ZnCO_3$ and $ZnSO_4$. A washing procedure for ZnS was therefore developed. The ZnS powder was mixed with Milli-Q water (deionized water that has been passed through an additional set of ion-exchange resins and an activated carbon filter). Dissolution of $ZnCO_3$ increased the pH of the mixture to approximately 9.5. The pH was slowly decreased by 20 μL additions of 0.1 M $HClO_4$ until an equilibrium was reached at pH 6. Eventually the suspension was centrifuged and the zinc concentration was determined in the supernatant by means of the atomic absorption graphite furnace technique. The whole washing procedure, including centrifugation, was performed in an inert N_2 atmosphere in a glovebox (VAC), and it was repeated until the Zn concentration in the supernatant leveled out at pH 6. The purity of the washed ZnS powder was confirmed with XPS and DR FTIR spectroscopy. The powder was stored under vacuum in a desiccator before usage. The specific surface areas of the adsorbents were determined with the krypton BET isotherms and were 6.9 and 4.1 $m^2\ g^{-1}$ for ZnO and ZnS, respectively. A second ZnS powder from Aldrich was also used. It contained less surface impurities and was, therefore, easier to wash. However, the surface area was only 0.5 $m^2\ g^{-1}$ and, as a consequence, it was only used for the high surface coverage samples (ZnS_{s2}, ZnS_{s3}) as described below.

Batch Titrations. Titrations in the presence of Co(II) and blank titrations (without Co(II)) were performed. These procedures were carried out with maximum protection against air. The solids were weighed and transferred to polypropylene or polycarbonate centrifuge tubes in a small glovebox under an argon atmosphere. Aqueous solution of 50 mM $NaClO_4$, prepared from distilled, boiled, and argon-sparged water, was added to each tube. The tubes were sealed with screw caps and several layers of ParaFilm, removed from the glovebox, and equilibrated on an end-over-end rotater for 18 h at 25 ± 0.5 °C. The pH was recorded in all tubes using a combination glass electrode (ROSS). Co(II) was added to half of the tubes, and equilibration was continued for an additional 6 h. The pH was thereafter adjusted to the desired value for each tube by 10 μL additions of 10 mM NaOH while the mixture was stirred vigorously with argon bubbling, and the tubes were finally equilibrated for another 24 h. The final pH values were registered, and the drift in pH was less than 0.01 unit/h. Solid/liquid separation was accomplished by centrifugation. The total Co and Zn concentrations in the supernatant were determined by means of the ICP−MS technique.

Table 1. XAS Sample ID's and Surface Coverages

sample ID	total [Co(II)]/μM	Co(II) % uptake	Co(II) surface coverage (μmol/m^2)
ZnO_{s1}	303	94.6	2.7
ZnO_{s2}	597	97.3	5.6
ZnS_{s1}	449	95.8	5.6
ZnS_{s2}	303	94.0	21.1
ZnS_{s3}	597	93.6	42.1

XAS Sample Preparation. Adsorption samples were analyzed as wet pastes. They were prepared according to the procedure described above for the batch titration. After completing the adsorption step, the suspensions were centrifuged, and ca. 98% by weight of the supernatant was removed; the total liquid volume was 31 ± 0.5 mL in all experiments. The wet pastes were transferred to 2 mm thick Teflon cells under nitrogen and subsequently were sealed with Mylar windows. The surface coverages of the samples studied by XAS together with the sample ID's used in the following text are listed in Table 1.

Data Collection. All XAS experiments were conducted on wiggler magnet beamline IV-2 at the Stanford Synchrotron Radiation Laboratory, with a ring energy of 3.0 GeV and a stored current of 50−90 mA. Data were collected using two flat Si(220) monochromator crystals, and the monochromator was detuned 50% at the highest scanning energy to minimize the transmission of higher order harmonics. One millimeter horizontal slits were used before the monochromator, and energy resolution was ~1.5 eV. The Co K-edge spectra of the adsorption samples were collected in the fluorescence-yield mode using a 13-element Ge solid-state array detector (Canberra) positioned at 90° to the incident beam. The energy calibration was monitored with a Co metal foil and an argon-filled ion chamber. The threshold energy was set as 7709 eV, which was chosen at the first inflection point of the Co K-edge. Multiple scans (12−16) were collected for each sample, and data were obtained out to $k = 13$ Å^{-1}, where k is the photoelectron wave vector referenced to the threshold of 7709 eV.

EXAFS Data Analysis. The extended X-ray absorption fine structure (EXAFS) region was isolated from each averaged X-ray absorption spectrum by standard procedures using the program package EXAFSPAK coded by G. George (Stanford Synchrotron Radiation Laboratory). The background absorption was removed by subtraction of the pre-edge region, which was fit with a third-order polynomial from ≈300 to 50 eV before the Co K-edge, and by fitting a four-region cubic spline function to the EXAFS region and subtracting it from the spectrum in order to define the edge jump and isolate the EXAFS. Normalization of the edge jump to a per atom basis was accomplished using McMaster coefficients.[13] The k^3-weighted EXAFS spectra were Fourier transformed over the k-range 2−12.2 Å^{-1} for all sorption samples using an unsmoothed window to yield the radial structure functions (rsf's). To minimize data cutoff effects, k_{min} and k_{max} were chosen in the nodes of the EXAFS function. In order to obtain quantitative information, EXAFS spectra were analyzed using a single-scattering, curved-wave formalism. Curve-fitting analysis of the data was carried out in two steps. First the peaks in the rsf corresponding to the first and second main shells were isolated and inversely Fourier transformed, and the inverse transforms were fitted separately. The r ranges for these transformations for Co/ZnO sorption samples were chosen approximately between 0 and 2.1 Å and 2.0 and 3.2 Å, depending on the location of nodes in the imaginary and absolute part of the rsf's; those for Co/ZnS were between 0 and 2.4 Å and 2.35 and 3.3 Å. It should be noted that because of insufficient

(10) Schindler, P.; Althaus, H.; Feitknecht W. *Helv. Chim. Acta* **1964**, *47*, 982.
(11) Licht, S. *J. Electrochem. Soc.* **1988**, *135*, 2971−2975.
(12) Bouwens, S. M. A. M.; van Veen, J. A. R.; Koningsberger, D. C.; de Beer, V. H. J.; Prins, R. *J. Phys. Chem.* **1991**, *95*, 123−134.
(13) McMaster, W. H.; Nerr del Grande, N.; Mallet, J. H.; Hubell, J. H. Rpt. UCRL-50/74, Section 2, Revision 1, Lawrence Livermore National Laboratory, Livermore, CA, 1969.

resolution the filtered first-shell contribution to the total EXAFS spectrum is contaminated by the second shell, and vice versa. In none of the data fits was the Brillouin–Nyquist limit on the number of free variables [$N_{free} = (2\Delta r_{filt}\Delta k)/\pi$][14] exceeded ($N_{free}$ = 13.6 and N_{free} = 7.8 for the first and second shell, respectively, of Co on ZnO; N_{free} = 18.2 and N_{free} = 5.8 for the first and second shell, respectively, of Co on ZnS). All phase-shift and amplitude data used to fit the experimental EXAFS oscillations were calculated with the theoretical EXAFS code FEFF version 5.04.[15,16] The theoretical single-scattering EXAFS functions for a Co–O correlation at 2.10 Å, denoted as Co–O_6, and a Co–Co correlation at 3.17 Å were calculated using the structure of crystalline $Co(OH)_2$ (pink, inactive form).[17] The differences in energy origin, ΔE_0, of the Co–O_6 and Co–Co functions were determined to be 2 and 6 eV, respectively, by fitting the experimental first- and second-shell EXAFS data from $Co(OH)_2$(s). These values were held constant whenever the functions were used in data fitting. Theoretical single-scattering EXAFS functions were also calculated for a Co–O correlation at 1.95 Å (denoted Co–O_4), a Co–S correlation at 2.30 Å, and two Co–Zn pair correlations at 2.80 and 3.95 Å. Structures of possible surface complexes were used as input files in these calculations. Due to the lack of experimental data, the ΔE_0-values could not be estimated and were therefore varied in the fitting procedure. The second step of the quantitative EXAFS analysis consisted of fitting the raw data. Coordination numbers and differences in energy origin, ΔE_0, were set to the values determined by fitting the isolated shells, and R and σ^2 were allowed to vary.

Results

Batch Titrations. Two parallel titration series were obtained for both of the adsorbents, one in the presence and the other in the absence of Co(II). The experiments were designed to yield a Co(II) coverage of 3 μmol/m^2 at 100% uptake on ZnO as well as on ZnS. Apart from studying Co(II) adsorption, the total Zn concentration in solution, with and without Co(II), was also monitored. The results are presented in Figure 1, parts a and b, for ZnO and ZnS sorbents, respectively. As can be seen, the Co(II) adsorption curves show the normal metal ion uptake behavior, i.e., increasing adsorption with increasing pH. The two Co(II) uptake curves are similar, the only difference being a slight displacement of the adsorption to higher pH values on the ZnS surfaces. However, the two systems behave differently with respect to Zn concentrations in solution. The total amount of Zn in the supernatant from the ZnO suspensions is not affected by the presence of Co(II). Although the scatter in the data is large, the expected increase of ZnO solubility with a decrease in pH is detected. On the other hand, the total Zn concentrations in the ZnS systems show a decrease in the presence of Co(II). This observation might be related to the colloidal properties of ZnS. In fact, the Zn concentrations in the blank experiment are too high, and similar findings were made in a recent study where elevated Zn concentrations were shown to be due to colloidal ZnS.[18] The apparent decrease in total Zn in solution in the presence of Co(II) is probably an effect of adsorption, which changes the surface charge and, therefore, the colloidal properties.

XANES Spectra of Co(II) at the Aqueous Solution–ZnO Interface. In Figure 2 Co K-edge X-ray absorption near edge (XANES) spectra and the corresponding second-derivative spectra of ZnO_{s1} (spectrum c) and ZnO_{s2} (spectrum d) are shown (see Table 1 for definition of the

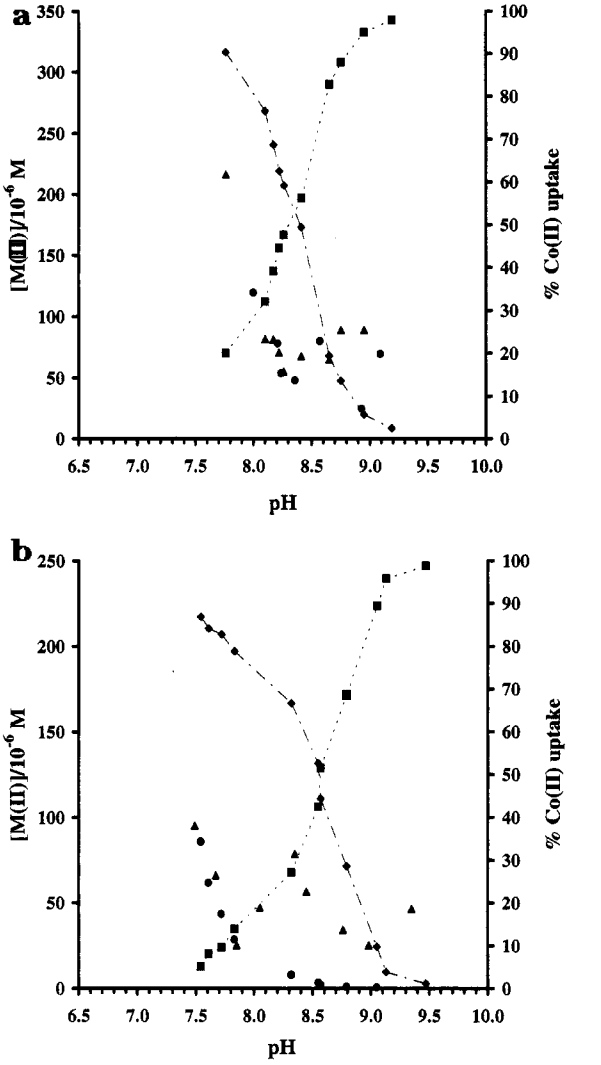

Figure 1. Adsorption of Co(II) on (a) ZnO and (b) ZnS. [Zn(II)] in (▲) absence and (●) presence of Co(II), (◆) [Co(II)], (■) percentage Co(II) uptake. Experimental conditions: (a) $[Co(II)]_{ini} = 4.15 \times 10^{-4}$ M, solid-to-liquid ratio = 20 g L^{-1}, ionic medium = 50 mM $NaClO_4$; (b) $[Co(II)]_{ini} = 2.40 \times 10^{-4}$ M, solid-to-liquid ratio = 19.5 g L^{-1}, ionic medium = 50 mM $NaClO_4$.

sample labels). For comparison, the spectra of unhydrolyzed aqueous Co(II) (spectrum a) and of solid $Co(OH)_2$ (spectrum b) are also included in Figure 2. Solid $Co(OH)_2$ was chosen for comparison because all samples were prepared at conditions close to the solubility of the hydroxide, and it is, thus, one likely surface product. The second-derivative spectrum Co(II)(aq) shows one sharp, intense peak at ≈7715 eV, which is typical of octahedral complexes.[19] A very weak pre-edge feature is present at ≈7698 eV which is assigned to a 1s → 3d transition. The spectra of $Co(OH)_2$(s) and the adsorption samples show additional peaks in the near-edge region relative to the spectrum of Co(II)(aq). This is probably due to scattering from second and higher coordination shells, which are not present in the aqueous solution of Co(II), and perhaps to contributions from multiple scattering in first-shell geometries different from octahedral. Theoretical studies of XANES spectra of first-row transition metal ions in aqueous solutions[20] and solids[21] have shown that the main

(14) Brillouin, L. *Science and Information Theory*, 2nd ed.; Academic Press, 1962.
(15) Rehr, J. J.; Mustre de Leon, J.; Zabinsky, S. I.; Albers, R. C. *J. Am. Chem. Soc.* **1991**, *113*, 5135.
(16) Mustre de Leon, J.; Rehr, J. J.; Zabinsky, S. I.; Albers, R. C. *Phys. Rev.* **1991**, *B44*, 4146.
(17) Lotmar, W.; Feitknecht, W. *Z. Kristallogr. Mineral. Petrogr. Abt.* **1936**, *A93*, 1144.
(18) Daskalakis, K. D.; Helz, G. R. *Geochim. Cosmochim. Acta* **1993**, *57*, 4923–4931.
(19) Della Longa, S.; Bianconi, A.; Palladino, L.; Simonelli, B.; Congiu Castellano, A.; Borghi, E.; Barteri, M.; Beltramini, M.; Rocco, G. P.; Salvato, B.; Bubacco, L.; Magliozzo, R. S.; Peisach, *J. Biophys. J.* **1993**, *65*, 2680–2691.
(20) Bianconi, A.; Garcia, J.; Marcelli, A.; Benfatto, M.; Natoli, C. R.; Davoli, I. *J. Phys.* C9 **1985**, no. 12, *46*, 101–106.
(21) Farges, F.; Brown, G. E., Jr.; Navrotsky, A.; Gan, H.; Rehr, J. J. *Geochim. Cosmoshim. Acta* (submitted).

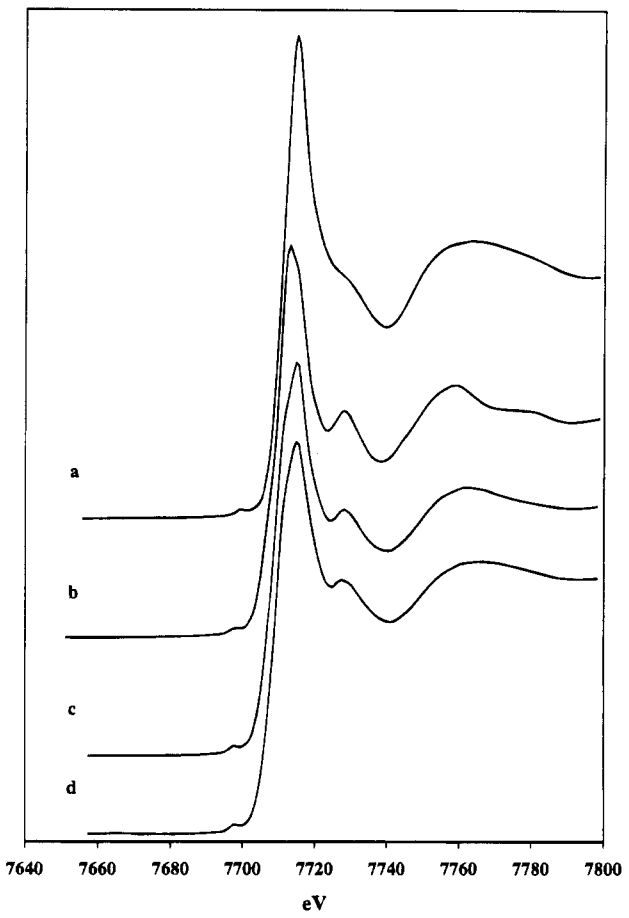

Figure 2. Co K-edge X-ray absorption edge spectra and the corresponding second-derivative spectra (′) of (a, a′) unhydrolyzed aqueous Co(II), (b, b′) $Co(OH)_2$ (pink inactive form), (c, c′) ZnO_{s2}, and (d, d′) ZnO_{s1}.

absorption edge can be accurately modeled by multiple scattering among first neighbors in the case of aqueous metal complexes, but involve significant multiple-scattering contributions from second-neighbor metals in crystalline solids and glasses.[21] Examination of the main K-absorption edge of Co in $Co(OH)_2$(s) and in the two Co/ZnO sorption samples (Figure 2) shows that the main absorption edge of the sorption samples has a feature on the low-energy side of the edge (≈7711 eV), resulting in a marked asymmetry, whereas the main edge of $Co(OH)_2$(s) is more symmetrical. These differences have also been observed in past XANES studies of Co sorption complexes at oxide–water interfaces vs $Co(OH)_2$(s).[4] Thus, the local average structures around Co(II) adsorbed on ZnO vs Co(II) in $Co(OH)_2$(s) must be dissimilar. One possible hypothesis for the observed asymmetry in the Co absorption edge in the sorption samples is the presence of two different first-neighbor coordination geometries for Co surface complexes (CoO_4 tetrahedra and CoO_6 octahedra). However, we can reject this hypothesis for the observed asymmetry, even though both coordination geometries are present (see EXAFS results below), because detailed analysis of EXAFS spectra of Co(II) chemisorbed on γ-Al_2O_3, α-Al_2O_3, TiO_2 (rutile), and $Al_2Si_2O_5(OH)_4$ (kaolinite)[4,5,22] shows that only CoO_6 octahedral sorption complexes are present, yet their Co K-edge spectra have the same asymmetry as observed for Co sorbed on ZnO. Instead, we suggest that this asymmetry is due to the presence of second-neighbor metal ions in the surface to which the Co is chemisorbed, i.e., Zn in the present case, and/or to static disorder effects in the oxygen nearest-neighbor coordination. This former assignment is consistent with the observation that the main Ti absorption edge in a variety of crystalline oxide model compounds and titanosilicate glasses shows two features which are caused by multiple scattering involving both the first-neighbor oxygens and second-neighbor metal ions around Ti.[21] If the second-neighbor ions were Co(II) arranged as in $Co(OH)_2$(s), we would not expect to see this type of asymmetry in the main absorption edge. Furthermore, if Co(II) were present mainly as an outer-sphere surface complex, these spectra would be expected to be similar to that of Co(II)(aq), which has a very symmetric main edge feature (Figure 2). This qualitative XANES analysis thus shows that adsorption of the major fraction of Co(II) on ZnO cannot be explained by precipitation of the binary hydroxide or by the formation of mononuclear outer-sphere surface complexes of Co(II).

It is interesting to note that the pre-edge feature at 7698 eV is slightly more pronounced in the sorption samples than in $Co(OH)_2$(s) and Co(II)(aq). All spectra were collected under the same experimental conditions; therefore, the observed differences are most likely not due to differences in the experimental procedure. Since the probability of this transition is related to the symmetry of the site, the intensity and energy of this feature are indicators of the coordination geometry of Co(II).[12,21] The 1s → 3d transition is symmetry forbidden for sites with O_h or D_{4h} symmetries, i.e., for sites with a center of symmetry. Upon lowering the symmetry to trigonal prismatic, D_{3h}, transitions to the xy and $x^2 - y^2$ d-orbitals become allowed. Consideration of appropriate molecular orbital diagrams suggests that only transition metal ions possessing D_{3h} symmetry with less than four d-electrons should have a substantial pre-edge peak. The same reasoning predicts that transition metal ions in C_{4v} or T_d sites should show pronounced pre-edge features if they have less than 8 or 10 d-electrons, respectively. The fact

(22) Towle, S. N.; Bargar, J. R.; Brown, G. E., Jr.; Parks, G. A.; Barbee, T. W., Jr. *Materials Research Society Proceedings, Vol. 357, Ceramic Interfaces* (in press).

that the intensity of the Co pre-edge peak increases slightly for the adsorption samples, together with the d^7 configuration of Co(II), indicates that a fraction of the adsorbed Co(II) ions has a coordination geometry close to square-pyramidal (C_{4v}) or tetrahedral (T_d).

XANES Spectra of Co(II) at the Aqueous Solution–ZnS Interface. The Co K-edge X-ray absorption near edge spectra and the corresponding second-derivative spectra of ZnS_{s1}, ZnS_{s2}, and ZnS_{s3} are shown in Figure 3 (see Table 1 for definition of sample labels). Also shown in this figure are the spectra of $Co(OH)_2$(s) and Co(II)(aq). Again the absorption edges of the sorption samples are different from those of the hydroxide and Co(II)(aq), indicating a different coordination geometry of the Co(II) ions adsorbed at the ZnS surfaces as compared to solid crystalline $Co(OH)_2$ and the octahedral hydrate. The lowest-coverage sample shows a relatively distinct pre-edge feature and, compared to the other two adsorption samples, the edge is broader and has a slightly different shape. This structural dependence on surface coverage is even more obvious in the second-derivative spectra. On the basis of the discussion above of XANES spectra of Co(II) chemisorbed on ZnO, the more pronounced pre-edge peak in the spectrum of the low-coverage sample suggests that a substantial fraction of the Co(II) ions chemisorbed on zinc sulfide has coordination geometries close to square-pyramidal or tetrahedral.

EXAFS Spectra of Co(II) at the Aqueous Solution–ZnO Interface. Background subtracted, k^3-weighted EXAFS spectra together with the corresponding radial structure functions of Co(II) at the ZnO surfaces are shown in Figure 4. Qualitative comparison of the EXAFS functions of ZnO_{s1} and ZnO_{s2} shows differences in the beat patterns, especially between 5 and 7.5 Å^{-1}. This implies that the local average structure of the Co(II) ions on ZnO is surface coverage dependent. Both rsf's show two dominating coordination shells. Each shell is, however, clearly composed of at least two atomic pair correlations. Differences in the rsf's of the two samples confirm the structural coverage dependence.

In the quantitative data analysis an attempt was first made to fit the filtered first shell of ZnO_{s1} with the $Co-O_6$ functions assuming an octahedral model, varying R and σ^2. The result is shown in Figure 5. As can be clearly seen, a poor fit above 7 Å^{-1} is obtained. Using the information extracted form the qualitative Co K-edge analysis, together with general knowledge of the coordination chemistry of Co(II) (see below), the data were instead fitted with two different Co–O correlations, one long, corresponding to a coordination number six, $Co-O_6$, and one short, corresponding to an assumed four-fold coordination, $Co-O_4$. The average difference in distance between six- and four-oxygen-coordinated Co(II) is ~0.16 Å, and the limit of resolution for the unfiltered EXAFS data, as approximated by $\Delta R = \pi/2\Delta k$, is 0.15 Å. Therefore, it should, in principal, be possible to resolve two discrete Co–O shells. In the fit, separate fractions of $Co-O_4$ and $Co-O_6$ were assumed, and accordingly, the coordination number of each pair correlation was calculated and systematically varied as $N(Co-O_6) = 6X_6$ and $N(Co-O_4) = 4X_4$, where X_6 and X_4 are the fractions of six and four coordinated Co(II), respectively. Apart from N, R, and σ^2, $\Delta E_0(Co-O_4)$ was also varied in the fitting procedure since no suitable data for calibration were available. The obtained fit shows great improvement in the high k region (Figure 5). Thus the first-shell data can be explained by the presence of Co(II) on ZnO coordinated to oxygen atoms at two different distances. The small remaining discrepancy between the data and the fit might be due in part to contamination by the second-neighbor shell.

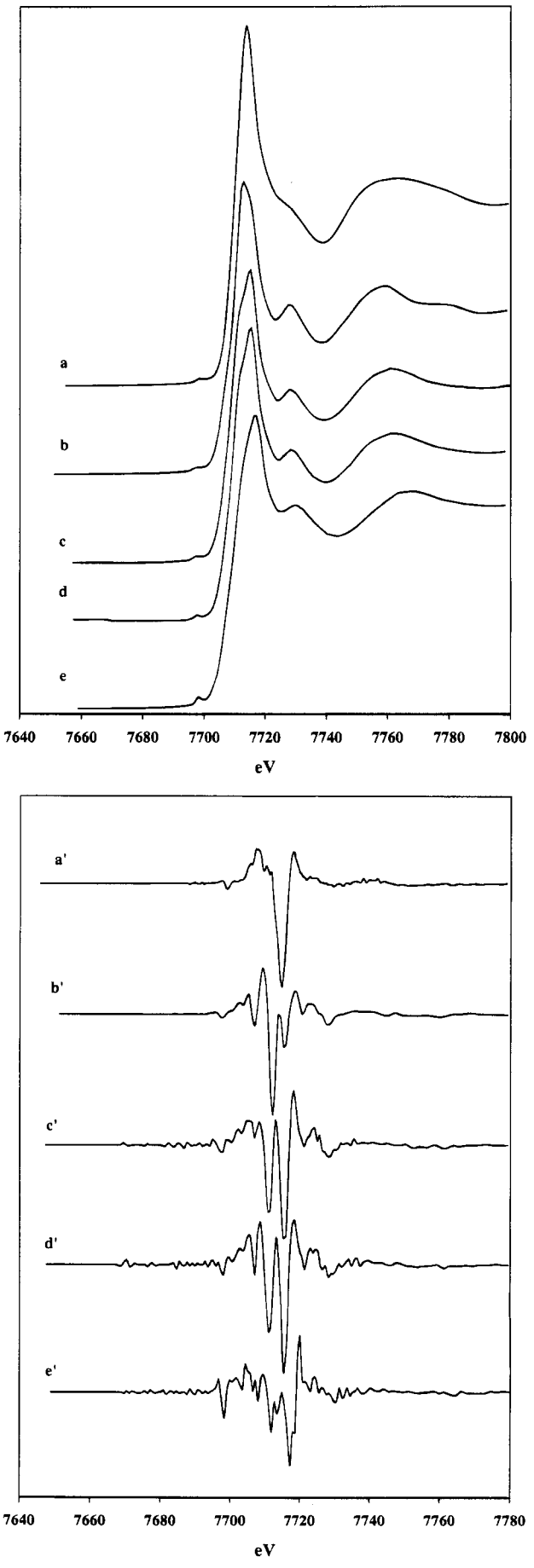

Figure 3. Co K-edge X-ray absorption edge spectra and the corresponding second-derivative spectra (′) of (a, a′) unhydrolyzed aqueous Co(II), (b, b′) $Co(OH)_2$ (pink inactive form), (c, c′) ZnS_{s3}, (d, d′) ZnS_{s2}, and (e, e′) ZnS_{s1}.

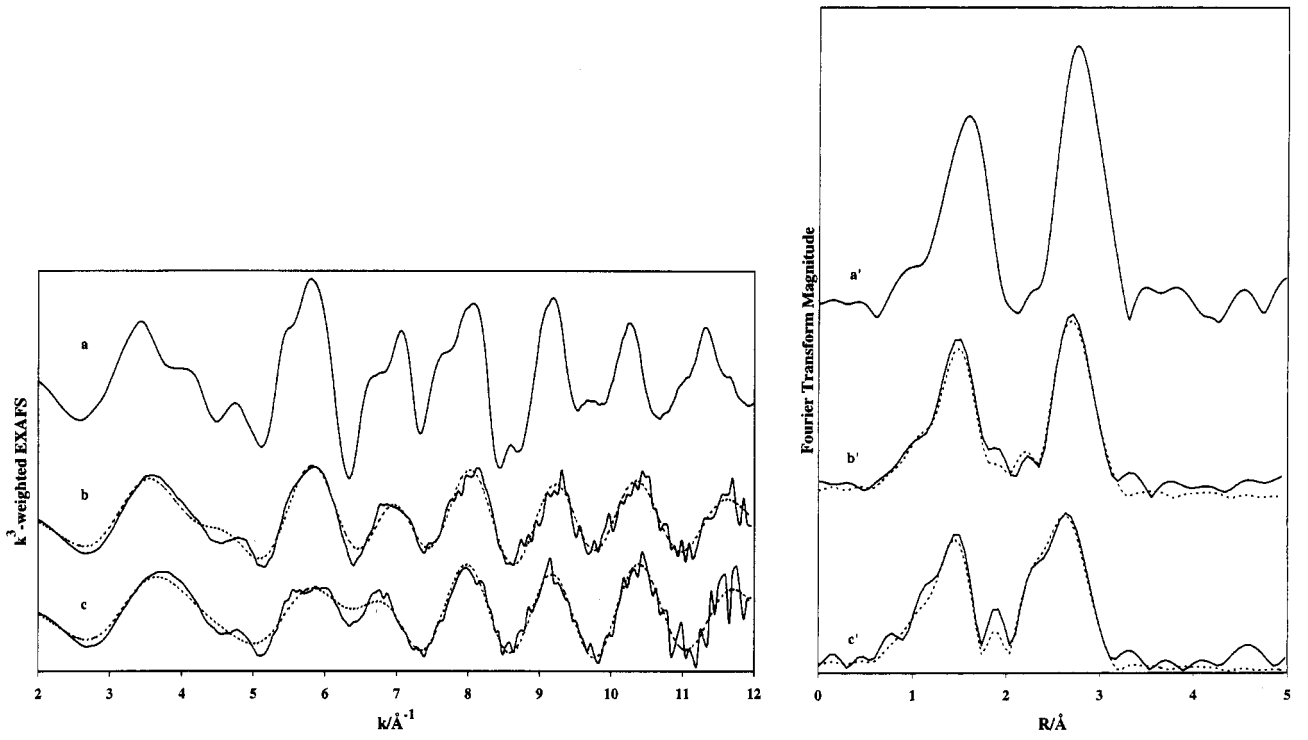

Figure 4. The k^3-weighted EXAFS and the radial structure functions not corrected for phase shift (′) of (a, a′) $Co(OH)_2$ (pink inactive form), (b, b′) ZnO_{s2}, and (c, c′) ZnO_{s1}. The dotted lines are the best fits obtained from the least-squares optimization procedure.

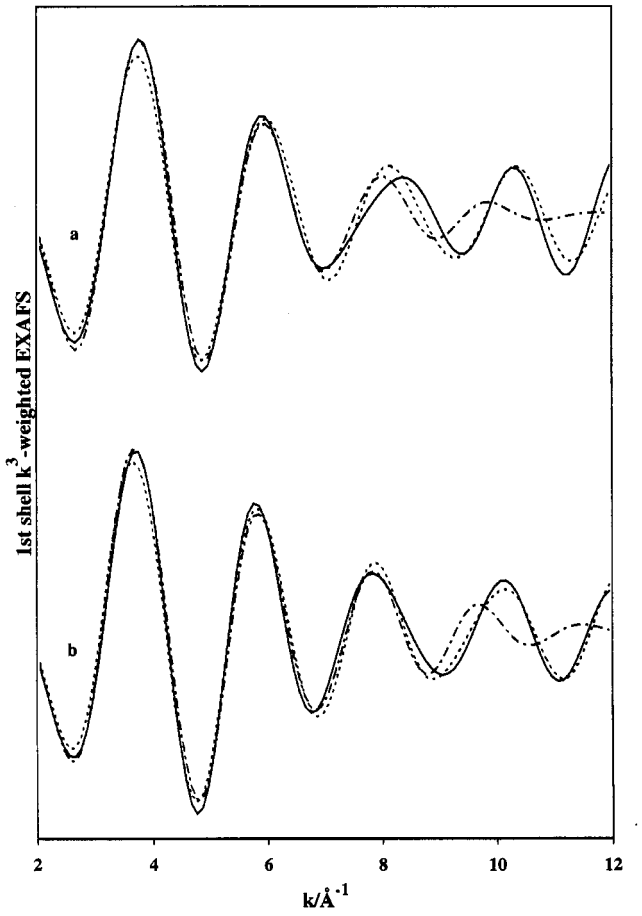

Figure 5. The least-squares fit of the Fourier filtered first shell (ΔR = 0–2.15 Å) of (a) ZnO_{s1} and (b) ZnO_{s2}. One model assumes Co–O_6 coordination (dot-dash) and the other fractions of Co–O_4 and Co–O_6 (dotted).

The similar backscattering properties of Co and Zn make refinement of higher shells more uncertain. Data reduction was constrained by making some basic assumption about the system, and the following criteria were used. The pair correlation at ~3.15 Å, which corresponds to Co–second-shell Co correlations in $Co(OH)_2$(s) and grows in significance with increasing Co surface coverage, was modeled as a Co–Co correlation. Other higher shell contributions, only significant at low coverage and not corresponding to distances in any known $Co(OH)_2$-phase, were fit with Co–Zn phase-shift and amplitude functions calculated using FEFF version 5.04. Fits of the second main shell of ZnO_{s1} with only Co and with both Co and Zn as backscatterers are shown in Figure 6. Clearly, the model is significantly improved when Co and Zn at 3.17 and 2.80 Å, respectively, are included. The optimization was carried out by varying N, R, and σ^2 and ΔE_0(Co–Zn). The number of second-neighbor Zn ions was systematically varied in 0.1 steps until a minimum in the χ^2 of the fit was found.

The described procedure was also used to analyze the first- and second-shell data of ZnO_{s2}, the only difference being that the ΔE_0 values for the Co–O_4 and Co–Zn correlations were set to those obtained above. The fits are graphically presented in Figures 5 and 6. The final fits of the raw EXAFS functions of both samples are shown in Figure 4 and the derived fit parameters are summarized in Table 2.

EXAFS Spectra of Co(II) at the Aqueous Solution–ZnS Interface. Background-subtracted, k^3-weighted EXAFS, together with the corresponding radial structure functions of ZnS_{s1}, ZnS_{s2}, and ZnS_{s3}, are shown in Figure 7. The EXAFS functions were isolated according to the procedure described above. There are obvious differences in the beat pattern in the region 5–10 $Å^{-1}$, especially between the lowest coverage sample and the two with higher surface loading. Thus, as was already noted in the qualitative XANES analysis, the local structure of Co(II) sorbed on the ZnS surface is also surface coverage dependent. The rsf's were calculated as the Fourier transforms of the k^3-weighted EXAFS spectra over the approximate k-range 2–12 $Å^{-1}$, depending on the location of the nodes of the oscillations. The first shell of ZnS_{s1} is comprised of two partly resolved peaks. The relative magnitudes of the peaks vary significantly with the order

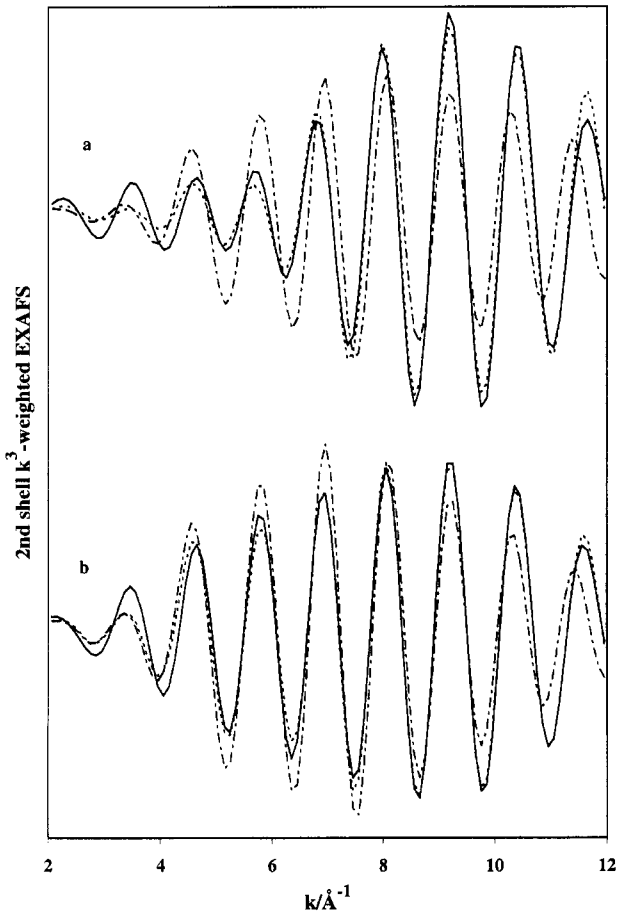

Figure 6. The least-squares fit of the Fourier filtered second shell ($\Delta R = 2.05-3.15$ Å) of (a) ZnO_{s1} and (b) ZnO_{s2}. One model assuming Co backscattering (dot-dash) and the other with backscattering from Co and Zn (dotted).

of k-weighting of the EXAFS function, indicating that they are the result of two different backscatterers.[23] At longer distances the rsf shows a symmetric second-shell peak at ≈2.8 Å and also a well-defined peak at ≈3.7 Å originating from a higher coordination shell. In contrast, the rsf's of ZnS_{s2} and ZnS_{s3} show different features. The first shell consists of a single slightly asymmetric peak while the second-shell peak once again is symmetric. In none of the rsf's is there any indication of a higher shell coordination.

Quantitative data were extracted from the EXAFS spectra following the general strategy already discussed. The rsf of ZnS_{s1} was Fourier transformed over the approximate r-ranges 0–2.4, 2.35–3.3, and 3.3–4.1 Å. Thus, the first two peaks were included in the same main shell because of insufficient resolution. Modeling the first-shell oscillations with either one or both of the Co–O_4 and Co–O_6 phase-shift and amplitude functions did not yield good fits (Figure 8). The agreement between the experimental data and the model, however, was improved greatly by including Co–S backscattering. The optimization was carried out by using Co–O_6 and Co–S phase-shift and amplitude functions, and R, σ^2, and ΔE_0(Co–S) were varied. The coordination numbers were initially arbitrarily set to 2, then both were varied systematically in 0.1 increments over the range 0–4 atoms until a minimum in the χ^2 of the fit was found. The resulting fit is shown in Figure 8 (dotted). The fact that the refined Co–O distance (2.00 Å) is intermediate between 1.95 and 2.10 Å, together with the pre-edge data, indicates the presence of four- and six-fold oxygen-coordinated Co(II) at the ZnS surfaces. Attempts were made to include both Co–O_4 and Co–O_6 phase-shift and amplitude functions in the refinements; however, with this many variables the least-squares fit did not result in unique fit values. The second shell is consistent with the presence of a coordination sphere of Co at 3.12 Å. It is notable that the refined Co–Co distance is slightly shorter than that for the Co(II) surface species on ZnO and in $Co(OH)_2$(s). The back-transformed higher shell peak was analyzed assuming a single-scattering process, and good fit was obtained with 1.5 Zn atoms at 3.93 Å. The phase-shift and amplitude functions were calculated with FEFF version 5.04, and refinement was performed by varying R, σ^2, ΔE_0, and the coordination number (stepwise in 0.1 increments).

The two higher coverage samples were analyzed in a similar manner. However, ΔE_0(Co–S) was fixed to the value obtained above, and the Co–Zn phase-shift and amplitude functions were omitted in the fitting procedure since no higher shell peak was present in the rsf's. Results of the final raw data fits are presented in Table 3 and Figure 7.

Discussion

Co(II) Adsorption at the ZnO–Aqueous Solution Interface. Adsorption of Co(II) at the aqueous solution–oxide and –clay interfaces has, as already mentioned, been studied using both macroscopic wet-chemical and spectroscopic methods. Co(II) shows a general adsorption behavior typical of a hydrated first-row transition metal ion, i.e., with an adsorption edge well below the pH of homogenous precipitation of the hydroxide phase and with a relative insensitivity to the PZC of the adsorbent.[24,25] The solid phases included in previous structural XAS investigations of Co(II) sorption are γ-Al_2O_3,[4] α-Al_2O_3,[22] TiO_2 (rutile),[4] SiO_2 (quartz),[8] and $Al_2Si_2O_5(OH)_4$ (kaolinite).[5,8] At all surface coverages considered in these studies, it was found that the first-coordination sphere consists of six oxygen atoms at ~2.1 Å in a slightly distorted octahedral arrangement, irrespective of the solid. Furthermore, analysis of coordination shells beyond the first strongly indicates that a major part of the Co(II) adsorption can be explained by the formation of bidentate inner-sphere surface complexes. All adsorbents studied also seem to induce polymerization of Co(II) at the surfaces. This is somewhat surprising since Co(II) shows only a very weak tendency to polymerize in aqueous solution.[26] The various oxides show some differences with respect to the extent of Co polymerization. At comparable surface coverages, smaller or more disordered surface polymeric species form on γ-Al_2O_3 and kaolinite than on quartz. Even smaller polymeric species form on TiO_2 (rutile). The effect of the different surfaces on the nucleation of larger hydroxo-bridged Co(II) polymers shows that the surface structure and/or the chemical composition influence the initial build-up of species beyond the first-coordination shell.

The macroscopic adsorption behavior of Co(II) on ZnO is similar to that described above, i.e., with a pronounced adsorption within a narrow pH range (Figure 1). However, the adsorption edge is shifted to somewhat higher pH values relative to previously studied oxides, which most probably is an effect of the higher adsorption density

(23) Sayers, D. E.; Bunker, B. A. In *X-ray Absorption: Principles, Applications; Techniques of EXAFS, SEXAFS, and XANES*; Koningsberger, D. C., Prins, R, Eds.; Wiley-Interscience: New York, 1988; pp 324–236.

(24) James, R. O.; Healy, T. W. *J. Colloid. Interface Sci.* **1972**, *50*, 53.

(25) James, R. O.; Healy, T. W. *J. Colloid. Interface Sci.* **1972**, *50*, 65.

(26) Baes, C. F., Jr.; Mesmer, R. E. *The Hydrolysis of Cations*; John Wiley & Sons: New York, 1976; pp 238–241.

Table 2. Structural Data for Co(II) Adsorbed on ZnO from Least-Squares Fitting of EXAFS[a]

	Co–O_4				Co–O_6				Co–Zn				Co–Co			
Γ	N	R	σ^2	ΔE_0	N	R	σ^2	ΔE_0	N	R	σ^2	ΔE_0	N	R	σ^2	ΔE_0
2.7	1.5	1.94	0.0024	−9	3.8	2.10	0.0107	2	1.1	2.80	0.0026	−15	3.0	3.17	0.0102	6
5.6	1.2	1.96	0.0010	−9	4.2	2.11	0.0083	2	0.5	2.81	0.0015	−15	5.4	3.15	0.0104	6

[a] The estimated maximum errors are $R \pm 0.02$ Å and N ● 25%. Γ is given in μmol/m^2, R in Å, and ΔE_0 in eV.

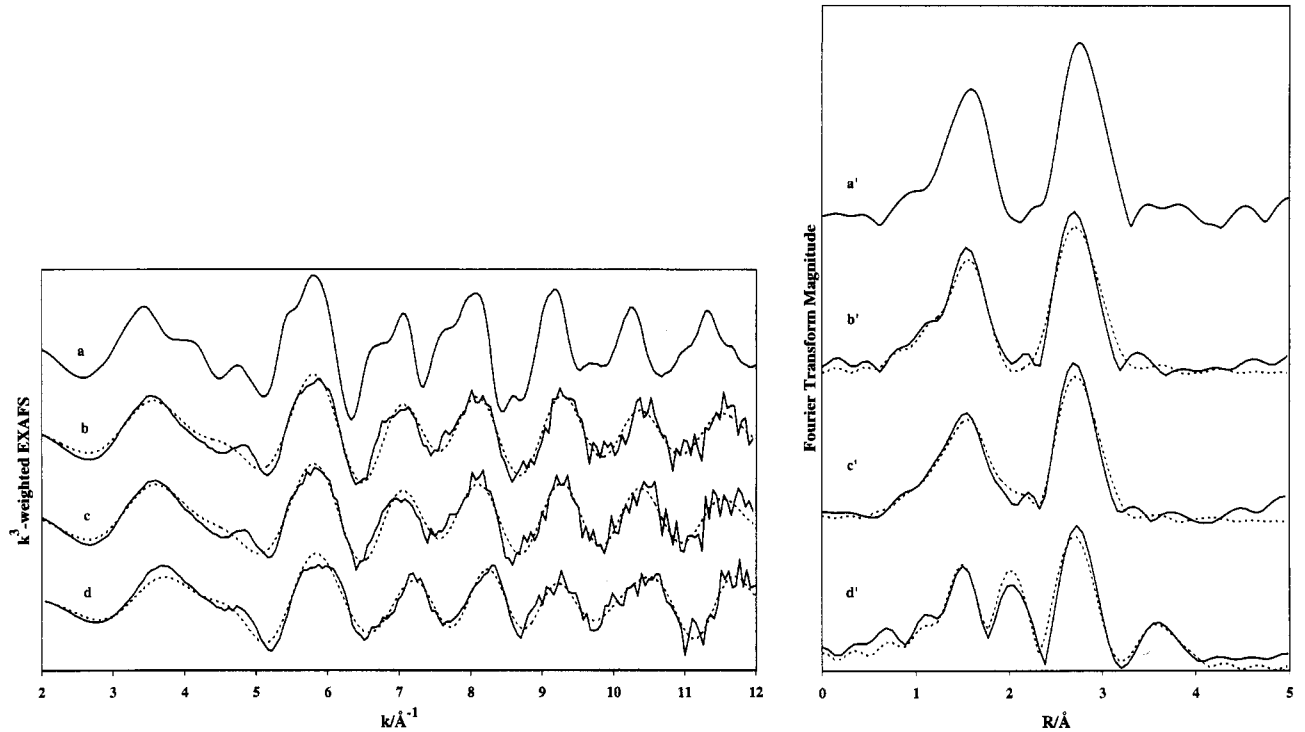

Figure 7. The k^3-weighted EXAFS and the radial structure functions not corrected for phase shift (′) of (a, a′) $Co(OH)_2$ (pink inactive form), (b, b′) ZnS_{s3}, (c, c′) ZnS_{s2}, and (d, d′) ZnS_{s1}. The dotted lines are the best fits obtained from the least-squares optimization procedure.

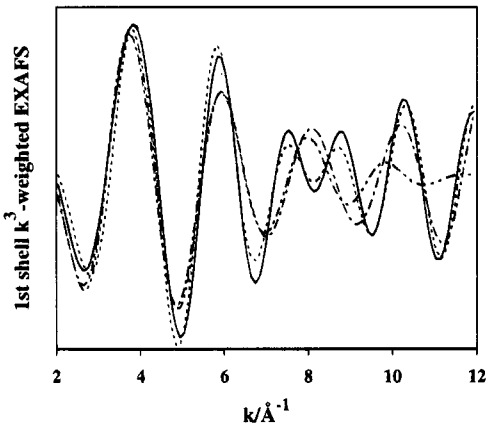

Figure 8. The least-squares fit of the Fourier filtered first shell (ΔR = 0–2.4 Å) of ZnS_{s1}, modeled with Co–O_6 (dot-dot-dash), fractions of Co–O_4 and Co–O_6 (dot-dash), and fractions of Co–O_6 and Co–S (dotted).

in the present study and perhaps also due to differences of the Lewis basicities of the SM–OH sites. The reason for the relatively high coverage is due to the fact that the ZnO powder used has a comparatively small surface area. Therefore, to have enough Co(II) on the surfaces for XAS measurements, we had to work with coverages >2.5 μmol/m^2, and the wet-chemical experiments were performed under similar conditions. Because of the shift of the adsorption edge, removal of Co(II) from the aqueous phase occurs in a pH region where $Co(OH)_2$(s) might be formed, either as a homogenous or a surface precipitate. If the availability of Co(II) in solution is controlled by the solubility of a particular Co(II)-bearing phase, the ion activity product (IAP) should equal the solubility product (K_s) of the phase formed (the activity of the phase is assumed to be 1). The following log K_s values have been reported for Co(II) hydroxide: −14.2 (blue form),[26] −14.8 (pink, active form),[26] −15.7 (pink, inactive form).[26] Thus, if either of these phases were formed during the titration, the log(IAP) of each experimental point should equal one of the listed values. The logarithms of the ion activity products for the experimental points presented in Figure 1 were calculated as $a_{Co}a_{OH}^2$, using the Davis equation to obtain the Co(II) activity coefficients. The results are shown in Figure 9 with log(IAP) plotted as a function of pH. Also included are the theoretical functions, as calculated by the computer program HYDRAQL,[27] corresponding to each of the homogenous hydroxide phases. Well below the pH of precipitation, the theoretical curves have a constant positive slope of 2. The function is given by log(IAP) = 2pH + log $a_{Co(II)}$ + 2 log K_w. This function is linear because there is no appreciable hydrolyses of Co(II) before precipitation of the pink inactive form, and therefore the log $a_{Co(II)}$ term is constant. The plot of log(IAP) as a function of pH for the experimental points does not follow the calculated curves. Between pH 7.7 and ~8.65 the slope is positive but decreasing, which shows that removal of Co(II) from solution in this pH region is not due to precipitation but most likely to surface complexation. The plot deviates from linearity since log $a_{Co(II)}$ is no longer constant but a function of adsorption, and, therefore, is influenced by factors such as surface coverage, surface potential, and magnitude of the stability

(27) Papelis, C.; Hayes, K. F.; Leckie, J. O. Technical Report 306, Department Civil Engineering, Stanford University, 1988.

Table 3. Structural Data for Co(II) Adsorbed on ZnS from Least-Squares Fitting of EXAFS[a]

	Co–O				Co–S				Co–Co				Co–Zn			
Γ	*N*	*R*	σ^2	ΔE_0	*N*	*R*	σ^2	ΔE_0	*N*	*R*	σ^2	ΔE_0	*N*	*R*	σ^2	ΔE_0
5.6	3.3	2.00	0.0072	2	1	2.36	0.0015	−8	4	3.12	0.0074	6	1.5	3.93	0.0047	−2
21.1	5.7	2.06	0.0117	2	0.4	2.37	0.0010	−8	4.5	3.15	0.0061	6				
42.1	5.1	2.07	0.0081	2					5.5	3.15	0.0075	6				

[a] The estimated maximum errors are $R \pm 0.02$ Å and $N \pm 25\%$. Γ is given in μmol/m², *R* in Å, and ΔE_0 in eV.

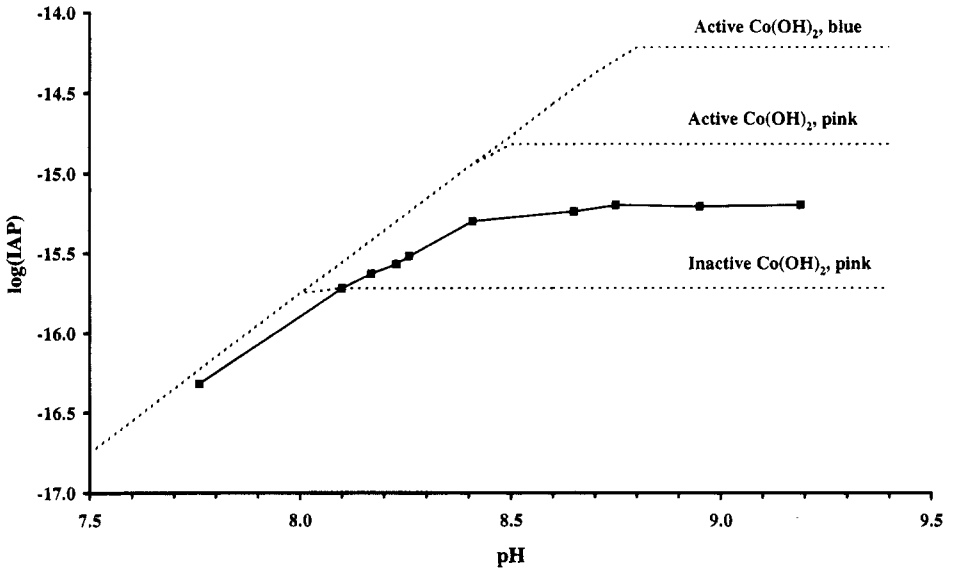

Figure 9. The log(IAP) of the experimental points in the Co(II)/ZnO batch titration calculated as $a_{Co(II)}a_{OH^-}{}^{-2}$ and plotted as a function of pH. The dotted lines are the corresponding values, calculated from tabulated thermodynamic data, of an aqueous solution of Co(II) with the total concentration of 4.15×10^{-4} M in equilibrium with the $Co(OH)_2(s)$ phases.

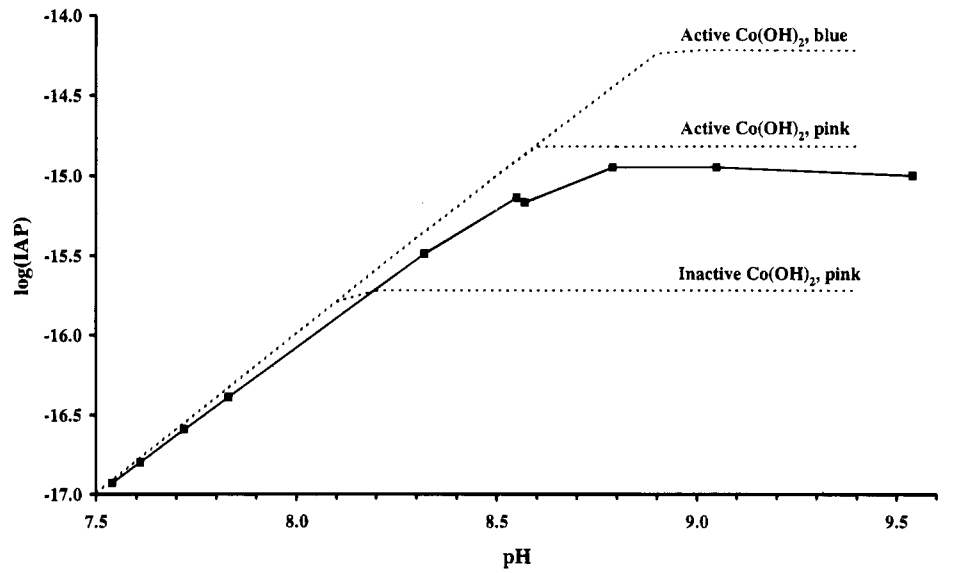

Figure 10. The log(IAP) of the experimental points in the Co(II)/ZnS batch titration calculated as $a_{Co(II)}a_{OH^-}{}^{-2}$ and plotted as a function of pH. The dotted lines are the corresponding values, calculated from tabulated thermodynamical data, of an aqueous solution of Co(II) with the total concentration of 2.40×10^{-4} M in equilibrium with the $Co(OH)_2(s)$ phases.

constants of the surface complexes. Above pH 8.65, the slope of the curve is close to zero, i.e., parallel to the abcissa, and thus the solubility of a hydroxide phase seems to control the Co(II) concentration in solution. The point where the slope changes from positive to zero indicates the pH where the adsorption process changes from surface complexation to precipitation, in this case 8.65. This is not, however, to be regarded as an abrupt change. At the conditions used in the titration, a pH of 8.65 indicates that surface complexation is responsible for 83% of the removal of Co(II) and a precipitated phase is responsible for the remaining 17% (see Figure 1). Since the maximum adsorption density in the titration is 3 μmol/m², the surface complex binding capacity of Co(II) on ZnO under the conditions of the experiment can be estimated to be 2.5 μmol/m². It is interesting to note that log K_s of the Co-containing phase accumulated on the ZnO surface is close to −15.2, which does not correspond to the solubility of any of the known Co(II) hydroxide phases. Although this might be due to experimental errors or to an error in the activity correction, it might also be due to a structural difference, caused by the ZnO surface, between the surface phase and the homogenous hydroxides.

The two samples of Co(II) adsorbed on ZnO analyzed by means of XAS were prepared at adsorption densities of 2.7 and 5.6 μmol/m². At equilibrium the log(IAP) values

for the aqueous phase were both −15.3, which is in close agreement with the log K_s of the Co(II) surface phase on ZnO discussed above. Using the value 2.5 μmol/m^2 as the maximum surface complex binding capacity of Co(II) on ZnO, it follows that theoretically 93% and 45%, respectively, of the Co(II) ions are present at the ZnO surfaces as complexes. Since the difference has structural implications, we would expect to see it in the XAS data. This expected structural surface coverage dependence has already been confirmed by comparison of the EXAFS functions and the rsf's. A more detailed discussion of the structure of Co(II) surface complexes on ZnO is presented below.

The quantitative first-shell data analysis clearly establishes the presence of Co(II) coordinated to oxygen at two distances. The refined distances agree very well with typical distances in four- and six-oxygen-coordinated Co(II) complexes/compounds, i.e., Co−O_4 at 1.95 Å and Co−O_6 at 2.10 Å. The vast coordination chemistry literature on Co(II) complexes shows that the two clearly dominating coordination numbers are in fact 4 and 6, and they are almost exclusively found in coordination geometries close to tetrahedral and octahedral, respectively.[28] Therefore, the most likely interpretation of the first-shell EXAFS data is that fractions of tetrahedral and octahedral Co(II) are present at the ZnO surfaces. This is the first case we are aware of where part of the hexaaquocobalt(II) ions are found to change coordination geometry at the aqueous−oxide interface. The phenomenon is not completely surprising since a small stability difference between tetrahedral and octahedral geometries has been reported for numerous Co(II) complexes; e.g., in aqueous solution $Co(H_2O)_6^{2+}$ is always in equilibrium with some $Co(H_2O)_4^{2+}$.[29] The relative preference of Co(II) for tetrahedral coordination can partly be explained by the fact that Co(II) has a d^7 electronic configuration. According to ligand field theory, d^7 will give a smaller energy difference between tetrahedral and octahedral coordination than any other d^n configuration, $1 \leq n \leq 9$. It is often difficult to determine what factors control the actual stereochemistry of Co(II). It is, however, clear that unidentate anionic ligands and more polarizable ligands favor a tetrahedral geometry.[30]

According to the wet-chemical analysis, a maximum of 93% of the Co(II) ions in the sample ZnO_{s1} are attached to ZnO as surface complexes, and the EXAFS data analysis gives 37% Co−O_4 and 63% Co−O_6. Although the uncertainties in coordination numbers are expected to be ~20%, it is quite unlikely, since Co−O_4 is most significant at low coverages (see below), that one coordination number is related to surface complexes and the other to a precipitated phase. Consequently, ZnO seems to have at least two types of surface sites, one which induces tetrahedral coordination and the other octahedral.

Higher shell analysis of ZnO_{s1} suggests the presence of Zn atoms at 2.80 Å. The assumptions used in the data reduction make the Co−Zn atomic pair more speculative. However, not only does the Co−Zn pair correlation satisfactorily explains this significant contribution to the total EXAFS, but it also is the most plausible according to the chemical reasoning above. A possible structural origin of the comparatively short Co−Zn distance is a bridging bidentate surface complex. The geometry of such a surface complex is depicted in Figure 11, where a Co(II) ion is coordinated at the edge of an oxygen-terminated surface, yielding a six-membered ring with the composition

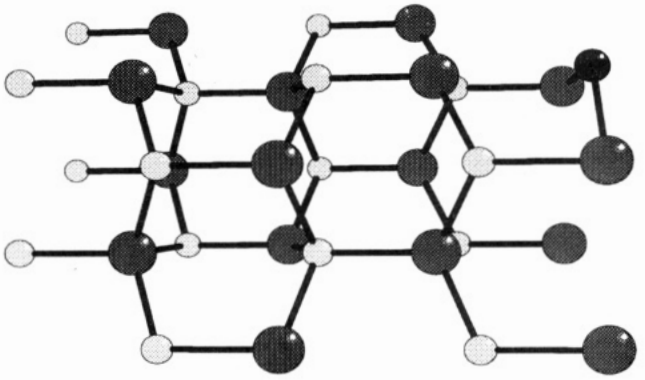

Figure 11. The proposed structure of a surface complex of Co(II) on ZnO, without additional water molecules, hydroxide ions, and protons: Co (black), Zn (shaded, small), O (shaded, large). $R_{Co-O} = 1.95$ Å, and Zn−O−Co and O−Co−O angles are 90° and 109.5°, respectively.

$CoZn_2O_3$. With the Co−O_4 distance derived from the EXAFS analysis, a Zn−O−Co angle of 90°, and assuming a noncontracted surface, the calculated Co−Zn distance matches the one experimentally determined. The Co−O_4 distance was used in the structural model since it maximizes the Zn−O−Co angle and since both the Co−O_4 and Co−Zn paths are associated with low surface coverage, i.e., with surface complexation (see below). When the proposed model is checked against the experimentally determined coordination numbers, it is clear that the number of Zn neighbors in ZnO_{s1} is rather high. However, with the inherently large uncertainties in these numbers (at least 20%), they do not contradict the suggested geometry. The presence of tetrahedral Co(II) and a Co−Zn correlation can thus be explained by adsorption to a bridging site. The proposed structure of the surface complex can be thought of as a continuation of the bulk structure, i.e., Co(II) adsorbs to a structural position where a Zn atom is missing. The only difference is a decrease in Zn−O−Co angle from tetrahedral to 90°. For some reason, the surface complex seems to gain a stabilizing energy by this decrease; however, it might also be an effect of accommodating the growing surface polymers.

The longest distance detected in the EXAFS analysis of ZnO_{s1} is due to Co−Co correlations at 3.17 Å, which is identical to a Co−Co distance in $Co(OH)_2$(s). However, the coordination number of the surface phase is markedly lower, 3 Co as compared to 6 Co in $Co(OH)_2$(s). As suggested by the titration data, 7% of the Co(II) ions on ZnO_{s1} are present as a precipitated phase. If this phase is close to $Co(OH)_2$(s) in local structure, the average coordination number (CN) would be $0.07 \times 6 = 0.42$. The higher number obtained from EXAFS analysis might indicate the formation of polynuclear surface complexes, similar to those observed in other systems, which should contribute to CN_{Co-Co}. These surface polymers constitute the smooth transition from smaller, isolated surface complexes to a surface precipitate defined by a constant log(IAP).

The difference between the ZnO_{s1} and ZnO_{s2} samples is, according to the wet-chemical results, a higher fraction of precipitate in the latter. Although there is a possibility of bulk precipitation, so far the precipitate has been assumed to be attached to the surfaces. This assumption is supported by several experimental observations. First, the log K_s of the precipitate in the presence of ZnO differs from either of the log K_s values of $Co(OH)_2$(s), and this might be an effect of the surfaces. Secondly, the EXAFS spectrum of ZnO_{s2} above 8.5 Å^{-1}, a region dominated by Co and Zn backscattering, differs markedly from that of $Co(OH)_2$(s). This implies a structural difference which is most likely induced by the ZnO surfaces. Here it should

(28) Carlin, R. L. *Transition Metal Chemistry* **1965**, *1*, 1−33.
(29) Cotton, F. A.; Wilkinson, G. *Advanced Inorganic Chemistry*, 4th ed.; John Wiley & Sons: New York, 1980; pp 768−773.
(30) Greenwood, N. N.; Earnshaw, A. *Chemistry of the Elements*; Pergamon Press: Oxford, 1986; pp 1312−1313.

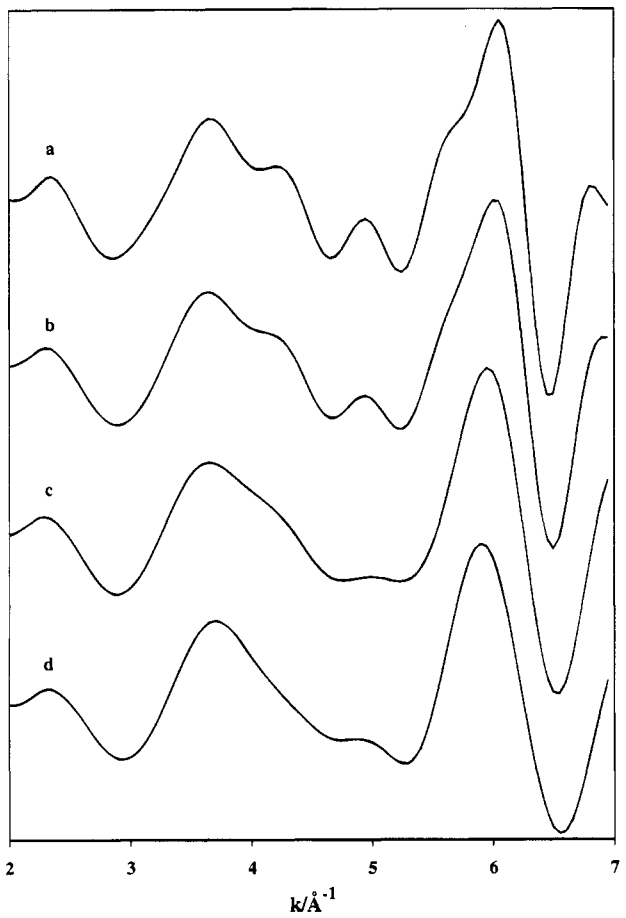

Figure 12. k^3-Weighted EXAFS functions from FEFF calculations of $Co(OH)_2$ clusters. (a) $r = 7$ Å, (b) $r = 6$ Å, (c) $r = 5$ Å, and (d) $r = 4$ Å.

be pointed out that the three different $Co(OH)_2$ phases have identical EXAFS spectra and thus identical local structures.[5] The structural mismatch between the surface precipitate and $Co(OH)_2$(s) is also evident in the low k-region. The EXAFS spectrum of the hydroxide shows a frequency at ~4 Å^{-1}, which is missing in the spectra of the two adsorption samples (Figure 4). To investigate the origin of this frequency a set of *ab initio* multiple scattering EXAFS calculations was performed with FEFF version 5.04. The atomic coordinates for the FEFF input files were extracted from the structure of $Co(OH)_2$(s). The X-ray absorbing atom was placed at the origin of a Cartesian system and the radial size of the clusters was varied. Clusters with radii of 4, 5, 6, and 7 Å where investigated, and the input files were constructed with the computer program ATOMS version 2.42.[31] The calculated EXAFS functions reveal that atoms beyond a radius of 4 Å need to be present for the feature to show up (Figure 12). This frequency receives contributions from a number of single- and multiple-scattering paths. This, together with the problem of unknown Debye–Waller factors, which were set to zero in the calculations, makes it difficult to assign the most significant scattering paths. It is clear, however, that scattering within the tri-atomic colinear arrangement of the absorber and additionally two Co atoms is important. The result of these calculations suggests that there is a structural difference between the surface precipitate and $Co(OH)_2$(s) beyond the first shell of Co atoms at 3.17 Å.

Comparison between ZnO_{s1} and ZnO_{s2} shows that the average structural environment of adsorbed Co(II) changes with increasing amounts of surface precipitate. The first-shell data of ZnO_{s2} show a decrease in the fraction of Co–O_4 and an increase of Co–O_6. Accordingly, the surface precipitate is comprised of Co(II) ions coordinated by six oxygens. This result, together with the decrease of CN_{Co-Zn}, supports the idea that the Co–O_4 and Co–Zn distances are related to surface complex formation. The most dramatic change is seen in the increase of CN_{Co-Co}, which shows the build-up of a surface precipitate resembling the local structure of $Co(OH)_2$(s). The surface phase should, however, only be regarded as "$Co(OH)_2$-like" because of the structural differences discussed above.

Co(II) Adsorption at the ZnS-Aqueous Solution Interface. Adsorption of metal ions at the aqueous solution–sulfide interface is usually explained by either a cation-exchange mechanism or surface complex formation. Metal ion adsorption through surface precipitation is also possible. At concentrations where surface precipitation can be neglected, the relative solubility of the sulfides determines which of the remaining two processes will dominate. Thus, comparison of K_s at the given experimental conditions for ZnS (wurtzite) and any likely cobalt sulfide phase should, in principal, reveal the adsorption mechanism, but there are many complicating factors. The wurtzite phase has recently been reported to be unstable in aqueous solution converting into the less soluble sphalerite phase.[18] The kinetics of the process are slow, and no conversion was detected using powder X-ray diffraction within the time frame of our experiments. Nevertheless, the conversion could conceivably have an effect on the adsorption processes. A number of cobalt sulfide phases have been identified,[32] but unfortunately the aqueous solubilities of these phases as a function of pH are not well-known. However, they are indicated to be of the same order as ZnS solubilities.[11] An *a priori* assignment of the adsorption mechanism based on relative solubilities is, therefore, not possible. Adsorption of Co(II) on CdS, which is slightly less soluble than the ZnS phases, has previously been studied using direct adsorption and electrophoretic mobility measurements.[33] It was found that Co(II) was adsorbed as surface complexes with an adsorption edge around pH 8, and the data were modeled with the surface equilibria

$$Co^{2+} + \underline{S}Cd\text{-}O^- = \underline{S}Cd\text{-}OCo^+$$

$$CoOH^+ + \underline{S}Cd\text{-}O^- = \underline{S}Cd\text{-}OCo(OH)$$

$$Co(OH)_2 + \underline{S}Cd\text{-}O^- = \underline{S}Cd\text{-}OCo(OH)_2^-$$

Thus, adsorption to sulfide sites was not included in the model.

The uptake of Co(II) on ZnS follows the same trend as adsorption on CdS and oxide surfaces. Again the relatively high surface coverages in the present study together with the possible different nature of the Lewis basicity sites displaces the adsorption edge to higher pH. Even compared to the Co/ZnO system at identical [Co(II)] to surface area ratios, adsorption occurs at slightly higher OH^- activities. This could indicate a lower overall affinity of Co(II) for ZnS or a smaller amount of active sites per square meter. The shape of the plot describing uptake as a function of pH (Figure 1) suggests that Co(II) is removed from solution through surface complexation or precipitation, and not cation exchange. This is concluded because cation exchange usually shows a relative insensitivity to pH. For example, Cu(II) clearly adsorbs on ZnS by cation exchange, and the extent of adsorption is about the same in the pH interval 4–8 at coverages even higher than 3 μmol/m^2.[34] Furthermore, this mechanism should show a stoichiometric (1:1) release of zinc into solution, which

(31) Ravel, B. ATOMS version 2.42c, University of Washington, 1994.

(32) Vaughan, D. J.; Craig, J. R. *Mineral Chemistry of Metal Sulfides*; Cambridge University Press: Cambridge, 1978.

was not observed in our titration (Figure 1). To distinguish between surface complexation and precipitation, the log(IAP) of $Co(OH)_2$ was calculated for each experimental point in the titration and plotted as a function of pH (Figure 10). As was the case for the Co(II)/ZnO system, the plot reveals two adsorption modes. Below pH ~8.75 Co(II) uptake seems to be controlled by surface complexation, and above this pH a slope of zero indicates a precipitation mechanism. The change from a positive slope to a slope of zero at 8.75, represents the crossover point between the mechanisms. Using the plot in Figure 1, it follows that a maximum of 67% of the Co(II) ions are removed as surface complexes. With a surface concentration of 3 μmol/m^2 at 100% uptake, the surface complex binding capacity of Co(II) on ZnS is calculated to be 2.0 μmol/m^2. This value is on the same order as the concentration of proton active sites on ZnS, determined potentiometrically to be 3.5 μmol/m^2.[35] Also, the site density on ZnS seems to be slightly lower than on ZnO (2.5 μmol/m^2), as was suggested by comparison of the uptake curves. It is interesting to note that the log K_s values of the precipitated Co(II) bearing surface phases in the ZnO and ZnS systems differ, perhaps indicating structural differences. The log K_s value of the phase on ZnS is closer to the solubility product of the pink inactive $Co(OH)_2$ modification.

Three samples with Co(II) surface coverages of 5.6, 21.1 and 42.1 μmol/m^2 were analyzed with XAS. With a maximum surface complex binding capacity of 2.0 μmol/m^2, these coverages correspond to 36%, 9%, and 5% of surface complex bound Co(II), respectively, and the EXAFS of ZnS_{s2} and ZnS_{s3} should therefore be dominated by the precipitated phase. The quantitative analysis of ZnS_{s1} yields an average first shell comprised of both oxygen and sulfur atoms. The Co–S distance is determined to be 2.36 Å, which is close to the Zn–S distance of 2.34 Å of wurtzite. Due to the complexity of the first main shell, the Co–O contact was fitted with one average distance at 2.00 Å. The pre-edge data indicate the presence of some tetrahedral Co(II), and the experimentally derived distance might therefore be explained by the coexistence of $Co-O_4$ and $Co-O_6$, resulting in an average distance of 2.00 Å.

Analysis of the well-resolved Co–Co shell gives $CN_{Co-Co} = 4$ and $R_{Co-Co} = 3.12$ Å. If the Co–Co correlation is assumed to originate from the precipitated fraction and there is a local structural resemblance between this phase and $Co(OH)_2$(s), the Co–Co coordination number can be calculated as $0.64 \times 6 = 3.84$, which is close to that obtained from EXAFS analysis. Consequently, these data are not consistent with the formation of any significant numbers of multinuclear surface complexes. The change from small size surface complexes to a surface precipitate, therefore, seems to be more abrupt on ZnS than on ZnO. The longest correlation determined by EXAFS analysis is Co–Zn at 3.93 Å, assuming a single-scattering process.

To get a clearer picture of the structures of Co(II) on ZnS, it is instructive to compare ZnS_{s1} with the two high surface coverage samples. EXAFS analysis of ZnS_{s2} and ZnS_{s3} reveals Co–O and Co–Co shells in close agreement with the local structure of $Co(OH)_2$(s). However, comparison of the EXAFS spectra in Figure 7 shows differences which might be related to differences of the longer range structures. A previous XAS study has shown identical EXAFS of the three possible homogenous precipitates of $Co(OH)_2$(s).[5] Therefore, a surface precipitate is the most likely explanation of these data, where the surfaces are

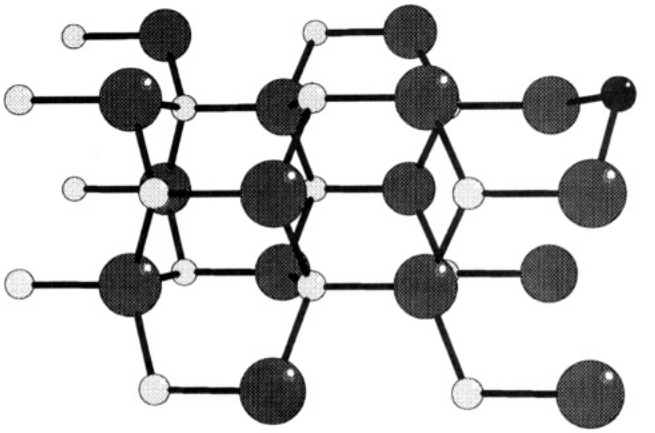

Figure 13. The proposed structure of a surface complex of Co(II) on ZnS, without additional water molecules, hydroxide ions, and protons: Co (black), Zn (shaded, small), S (shaded, large). $R_{Co-S} = 2.36$ Å, and Zn–S–Co and S–Co–S angles are both 109.5°.

causing structural disorder as compared to the known cobalt(II) hydroxide phases. The FEFF calculations of various sized $Co(OH)_2$ clusters discussed above further support this interpretation. The missing frequency at 4 $Å^{-1}$ in the spectra of the adsorption samples is strong evidence for a structural mismatch beyond the first shell of Co atoms as compared to $Co(OH)_2$(s). It is notable that this effect exists even at the high coverage of 42.1 μmol/m^2.

The structural results for ZnS_{s2} and ZnS_{s3} also provide indirect clues about the structures of the surface complexes. Because of the inverse relationship between the significance of the Co–S and Co–Zn correlations and surface coverage, as shown by the data in Table 3, it is clear that these correlations are related to comparatively low Co(II) surface coverage. Also, the average Co–O distance is significantly shorter and the pre-edge peak is more intense at lower coverage. The structural elements Co–S (2.36 Å), Co–Zn (3.93 Å), and a short Co–O distance are accordingly all possible components of surface complexes. It follows from the titration data that there is no likelihood of cation exchange, which would result in the formation of a three-dimensional cobalt sulfide phase. The Co–S contact is therefore a result of a surface coordinative interaction. The experimentally determined average Co–S coordination number of 1 gives an actual coordination number of 2.8 (=1/0.36) if all surface complexes were formed at sulfide sites. Therefore, even with the large errors in the coordination numbers from EXAFS analysis, a monodentate coordination seems unlikely. The Co–S and Co–Zn correlations can be explained by a bridging coordination of Co(II) to two sulfur atoms at the edges of the S-terminated (001) surface (Figure 13). A noncontracted surface, a Zn–S–Co angle of 109.5 (tetrahedral), and a Co–S distance of 2.36 Å yields the Co–Zn distance of 3.85 Å, in reasonable agreement with the distance obtained from EXAFS analysis. Similar to Co(II) on ZnO, the proposed surface complex can be regarded as a continuation of the bulk structure, with Co(II) occupying structural positions of missing surface Zn atoms. However, on ZnS fewer structural distortions are observed. There are alternative interpretations of the short Co–O distance. It could be associated with a specific type of SZn–OH site, inducing 4-fold coordination of Co(II), as was suggested for ZnO. Another possible origin of a Co–O distance typical of four-coordination is a mixed-ligand surface complex. A coordination of Co(II) to surface sulfide sites means an interaction between Co(II) and a ligand of a polarizable character. As suggested, these complexes are expected to have tetrahedral symmetry. Since they

(33) Park, S. W.; Huang, C. P. *J. Colloid. Interface Sci.* **1989**, *128*, 245–257.
(34) Persson, P.; Parks, G. A.; Brown, G. E., Jr., manuscript in preparation.
(35) Rönngren, L.; Sjöberg, S.; Sun, Z.; Forsling, W.; Schindler, P. W. *J. Colloid. Interface Sci.* **1991**, *145*, 396–404.

necessarily have to have a mixed first coordination shell of O and S atoms, the complexes should be characterized by a comparatively short Co–O distance.

To summarize, surface complexes of Co(II) are formed on ZnS at coverages lower than ~2.0 μmol/m^2. There is a direct bond between Co(II) ions and sulfur atoms at the surface, with Co(II) adsorbing to sulfide ions in sites of tetrahedral symmetry. Some surface complexes display a short Co–O bond characteristic of 4-fold coordination. This can be related either to coordination at specific $\equiv$SZn–OH sites or to mixed S and O ligand surface complexes. At higher coverages, a structurally disordered "cobalt hydroxide like" surface precipitate is formed. The disorder is observed even at very high Co(II) uptake.

Concluding Remarks

The main objectives of the present study were to examine the effects of substrate composition and structure on adsorption. In this respect, the ZnO and ZnS surfaces do not seem to change the overall macroscopic adsorption behavior of Co(II) in any dramatic way, as evidenced by the shape and position of the adsorption edge. The wet-chemical results, presented in the form of log(IAP) vs pH diagrams, reveal some minor differences between ZnO and ZnS. These are seen in the shape of the graphs, the apparent log K_s values of the surface precipitate, and the estimated Co(II) maximum surface complexing capacities of the adsorbents. The deviations in graph shape and log K_s is a direct result of differences in the aqueous Co(II) activities, which, in turn, might be related to differences in Co(II) surface speciation on ZnO and ZnS, respectively. The two observed adsorption capacities are also a reflection of the surface properties of the adsorbents. Here, the larger size of the sulfide ion probably plays an important role since the capacities are expressed in μmole per area unit.

At the microscopic level, ZnO and ZnS show a somewhat different behavior as compared to the previously studied oxide and clay minerals. Perhaps the most important finding of this work is the spectroscopic evidence for surface complexes with a short Co–O bond, presumably four-coordinated Co(II). ZnO and ZnS are the only surfaces reported to date to cause a geometric and stoichiometric change of the first coordination sphere of hydrated Co(II). This phenomenon is of general interest since a coordination change of an adsorbed metal ion at a surface will change both its hydrolysis and its general chemical reactivity.

Finally, we believe that this study has shown the applicability of X-ray absorption spectroscopy to investigations of metal ions at the aqueous solution–sulfide interface. Without the EXAFS analysis, it would not have been possible to show, in a direct way, that Co(II) adsorbs as surface complexes to sulfide sites. The XAS technique will clearly be an important tool in future studies of the aqueous surface chemistry of metal sulfides.

Acknowledgment. Thanks to B. Hedman, Stanford Synchrotron Radiation Laboratory, for technical support, and members of the Surface and Aqueous Geochemistry Group, Stanford University, for help with data collection. The Swedish Natural Science Research Council is acknowledged for financial support of P.P. as is the U.S. Department of Energy through grant DE-FG03-93ER14347 (G.E.B. and G.A.P.) and an NSF-MRSEC grant through the Stanford Center for Materials Research (G.E.B.). The XAS work was carried out at SSRL, which is supported by the Department of Energy, Office of Basic Energy Sciences, the NIH, Division of Research Resources, and DOE, Office of Health and Environmental Research.

LA9502507